ROBUST NONLINEAR ADAPTIVE IMAGE RESTORATION IN LAND MINE DETECTION PROBLEM

Z D Hrytskiv*, S V Voloshynovskiy*, A R Allen#

***State University "Lvivska polytechnika", Ukraine**
#University of Aberdeen, Scotland, UK

INTRODUCTION

The application of modern sensor technologies makes it possible to solve a wide range of applied problems. However, in most cases the quality of primary radar and radiometry images is far from desirable for unequivocal data interpretation and object recognition. This considerably decreases the possibility of using such systems in the solution of the problem of safe mine removal. Among the main factors, that reduce image quality and decrease probability of correct detection and confidence level, are the spatial blurring effects of imaging systems and noise of different types. The main blurring factors, that lead to ambiguity of measurement, are finite imaging aperture, sparseness of aperture resulting in large side lobes in a directional antenna pattern, and nonoptimal beamforming caused by phase errors in aperture. These lead to a decrease in plan resolution. Additionally, the situation is complicated by errors of measurement or noise in the receiver and data acquisition system, which can be modeled by additive Gaussian noise. In many cases, the received data is nonuniformly sampled owing to failures in the spatial scanning system or the physical nature of possible spatial sampling, resulting in information loss. The last two distortions can be represented by impulse noise on the basis of the "salt and pepper" model.

To enhance image quality, deconvolution is often used as an alternative to additional measurements. This relates to solution of an inverse ill-posed problem, and consists in mathematical compensation for the degradation using image restoration and noise suppression methods. The aim of this paper is to demonstrate the advantages of the proposed robust estimation strategy in the restoration of low-contrast radiometry images, and its possibilities regarding mine detection in an environment of objects with similar form and dimensions. The paper presents a robust approach to image restoration that combines the properties of classical regularized iterative algorithms and robust features based on the concept of **M**-estimators. The proposed technique could be efficiently used for the solution of the depth resolution enhancement problem in radar applications.

MODEL OF IMAGING SYSTEM

Image degradation caused by blurring and image contamination with Gaussian and impulse noise, can be represented by the following model:

$$g = \begin{cases} Hf + n, \text{ with probability } 1 - p, \\ g_{\min}, \text{ with probability } p / 2, \\ g_{\max}, \text{ with probability } p / 2 \end{cases} \quad (1)$$

where g represents the degraded image and n is a Gaussian noise component. H represents the linear spatially invariant blurring operator and f denotes the original image. $g_{\min}$ and $g_{\max}$ are the minimum and maximum values of the image dynamic range.

RESTORATION ALGORITHM

Despite the variety of approaches to the restoration problem, it can be formulated in general as the estimation or retrieval of the original image from the degraded image using available *a priori* information about the model of observation (1), the blurring function, the noise statistics, and the original image (given in the form of image smoothness, solution constraints on some specific image features, and parametric image models). This involves the solution of inverse problems which are known to be ill-posed. According to the nature of *a priori* information used and the estimation strategy, i.e. *minimum mean square error* (MMSE) or *least squares error* (LSE) estimators, the methods can be divided into *stochastic* and *deterministic*. If only information about image smoothness is used, the methods are supposed to be *linear* ones, and *nonlinear* if specific image features such as nonnegativity or finite extent are included in a compound function as constraints. Linear methods are unable to solve the extrapolation problem, and thus cannot increase spatial resolution. Therefore, only nonlinear methods are further considered in this paper. However, if there is some uncertainty regarding these constraints, such as errors in blurring operator definition or variation of the real noise statistics from those assumed typical for radar and radiometry imaging problems, then the above approaches fail to restore the image uniquely. The above problem can be effectively solved by means of robust estimators such as **L**-, **R**- or **M**-estimators. The second problem of image restoration is in global assumptions about the image behaviour which suggest stationarity in stochastic approaches and smoothness in deterministic ones. The approach used in this paper refers to the deterministic group of methods, and to overcome this drawback a spatially adaptive approach using a *modified noise visibility function* is proposed.

Since classical regularized algorithms based on *LSE* approach fail to restore images in the presence of impulse noise, a robust estimation strategy using an **M**-estimation approach is used: this is considered in the next section.

Robust adaptive restoration based on M-estimation

The robust estimation problem based on **M**-estimation concept with constraint on image smoothness is formulated according to the criterion

$$\min_{\hat{f}} \Phi[\hat{f}] = \rho(g - H\hat{f}) + \alpha\|C\hat{f}\|^2 \qquad (2)$$

where $\rho(.)$ is a robust positive-definite objective estimation function, $\|\|$ is matrix norm, C is a high-pass filter, and α is a regularization parameter. In many practical situations, the minimization problem is solved by converting (2) into a weighted least squares problem which is then handled by available subroutines. The weights depend on the assumed objective function and the noisy data. In order to take into account information about local features of the restored image we propose to modify the above minimization problem:

$$\min_{\hat{f}} \Phi[\hat{f}] = \rho_W(g - H\hat{f}) + \alpha\|C\hat{f}\|^2 \qquad (3)$$

where $\rho_W(.) = w\rho(.)$ is a weighted objective function with weight coefficients w of a diagonal matrix W which are connected with image pixels and define spatial image activity. Therefore, the problem of adaptive robust image restoration consists in: (i) proper choice of objective function, determined by *prior* assumptions about the noise distribution, and (ii) definition of an adaptation strategy that takes into account *"prior"* knowledge of local structure of the restored image and is calculated using a modified *noise visibility function*.

Objective function. The application of steepest descent algorithms to the solution of the minimization problem (3) results in the iterative scheme

$$\hat{f}^{k+1} = \hat{f}^k - \beta\, d\Phi[\hat{f}^k]/d\hat{f}^k \qquad (4)$$

where $\hat{f}^{k+1}$ is the estimate of f on k+1 iteration, β is a relaxation parameter that controls the convergence rate, and

$$\frac{d\Phi[\hat{f}]}{d\hat{f}} = -2H^T W\Psi(g - H\hat{f}) + 2\alpha C^T C\hat{f} \qquad (5)$$

where $\Psi(r) = d\rho(r)/dr$ is an *influence function* and $r = g - H\hat{f}$ is the residual, "T" denotes matrix transpose. In classical restoration approaches, the residual is assumed to have a normal distribution due to the assumption of additive Gaussian noise in model (1). In this case a *LSE* estimator is used

$$\rho(r) = \frac{1}{2}r^2 \quad \text{and} \quad \Psi(r) = r. \qquad (6)$$

However, model (1) includes not only additive Gaussian noise, but also an impulse component. Depending on the nature of the impulse noise the following objective functions are chosen in practice (see Press et al (1)):

- for *double or two-sided* distribution

$$\rho(r) = |r| \quad \text{and} \quad \Psi(r) = \mathrm{sgn}(r) \qquad (7)$$

- for *Lorenzian* distribution

$$\rho(r) = \log\left(1 + \frac{1}{2}r^2\right) \text{ and } \Psi(r) = \frac{r}{1 + \frac{1}{2}r^2}. \qquad (8)$$

"Salt-and-pepper" impulse noise is not directly described by means of such distributions, because it has more intensive "tails". The typical histogram distributions of a low contrast original image, blurred image, blurred and noisy image according to model (1), and residual, are shown in Figure 1a,b,c,d, respectively. We propose a generalized *influence function*

$$\Psi(r) = \frac{r}{1 + \left(\frac{r}{\theta}\right)^{2\upsilon}} \qquad (9)$$

With the correct choice of parameters θ and υ, which determine the break-point in the function to reduce the influence of large residual values, all the above types of impulse noise could be effectively removed. The use of such influence functions was proposed by Voloshynovskiy et al (2) applied to image restoration problems in high resolution radar imaging systems. The objective and influence functions for the *LSE* and proposed ($\theta = 35$, $\upsilon = 5$) estimators are shown in Figures 2 and 3, respectively.

The resulting iterative algorithm, that minimizes (3) for the *influence function* considered above and constraints on solution, is

$$\hat{f}^{k+1} = C_S\Re[\hat{f}^k] + \beta H^T W\Psi(g - H\Re[\hat{f}^k]) \qquad (9)$$

where operator $C_S = I - \alpha\beta C^T C$ represents a low-pass filter that smoothes the restored image to prevent noise fluctuations in the solution and is a soft constraint on smoothness. $\Re$ is the projection operator onto the convex set of nonnegative solutions and solutions with the given properties of amplitude image spectrum

$$\Re = C_N C_M \qquad (10)$$

where C_N is constraint on nonnegativity of the solution and C_M is constraint on *a priori* given model of the solution. Unfortunately, constraint C_M is not directly available in many practical applications. Therefore, a parametric model in the frequency domain proposed by Hrytskiv and Voloshynovskiy (3) is used that takes into account the spatial anisotropy of real image spectra. The upper bound of the restored image model is determined by constraint on smoothness of solution and the above constraint determines the lower bound. The use of this constraint effectively removes *ringing effects* in the restored image.

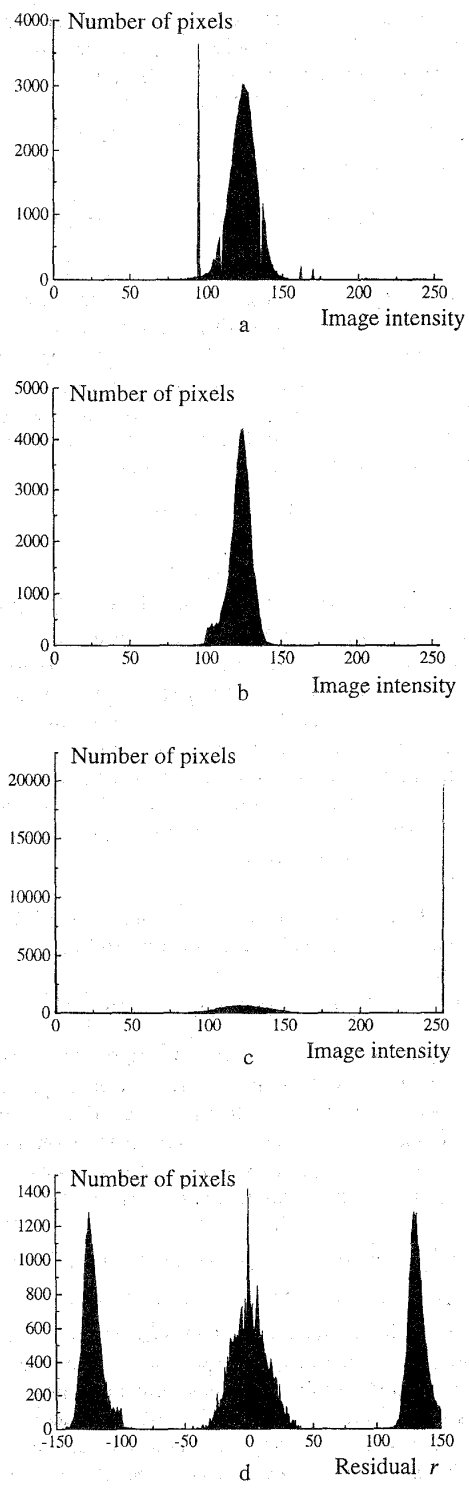

Figure 1: Histogram distributions of (a) original image f, (b) blurred image Hf, (c) blurred and noisy image g, (d) residual r

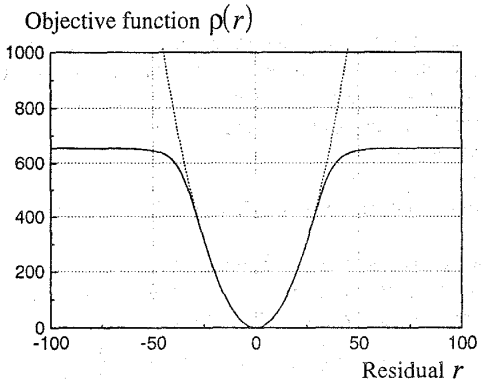

Figure 2: Objective functions of *LSE* and proposed estimators shown in dotted and solid lines, respectively

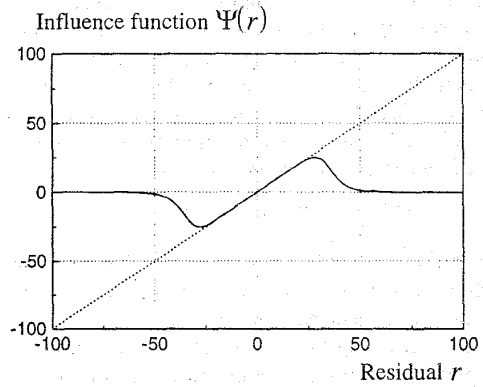

Figure 3: Influence functions of *LSE* and proposed estimators shown in dotted and solid lines, respectively

Adaptation strategy. The key point of the adaptation strategy is calculation of a *noise visibility function*. The role of the noise visibility function in our formulation is to mathematically express regions of high spatial image activity that correspond to edges and fine details in the image, and low activity associated with flat areas. In the case of hard thresholding, this could be expressed as

$$NVF = \begin{cases} 0, & if \quad f \in R_e, \\ 1, & if \quad f \in R_f, \end{cases} \tag{11}$$

where R_e is an edge region and R_f is a flat area, which are determined using an edge detection operator or local image variance. We propose to use a *modified NVF* based on fuzzy logic, using a sigmoid function to obtain a robust estimation of the above regions

$$NVF = \frac{1}{1 + exp\left(-\gamma\left(\sigma_f^2 - L\right)\right)} \tag{12}$$

where γ describes the degree of fuzziness and parameter $L = \left(\sigma_{max}^2 - \sigma_{min}^2\right) / d$ determines the shift of activation function between maximum and minimum

values of partially restored image variances σ^2_{max} and σ^2_{min} on k iteration. It was experimentally established that a good compromise between noise activation and edge connectivity could be achieved for $\gamma = 0.01$ and $d = 35$. Thus, threshold L depends on maximum and minimum image variances and is selected adaptively to each image. The activation function used in (12) for *NVF* calculation is depicted in Figure 4.

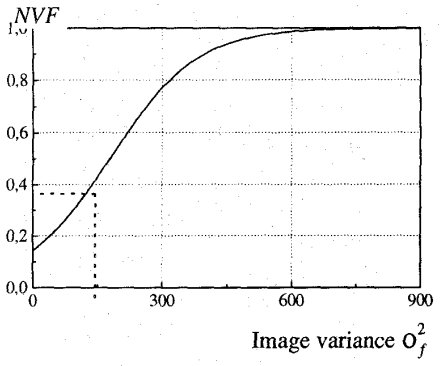

Figure 4: Activation function for *NVF* calculation

RESULTS OF COMPUTER SIMULATION AND CONCLUSIONS

This section demonstrates the main properties of the proposed robust restoration algorithm in comparison with classical techniques. The comparison measure is defined according to SNR between original image f, degraded image g and restored image f^k

$$\delta_{\hat{f}} = \frac{\|f - \gamma\|}{\|f\|} \tag{13}$$

$$SNR = 10\log_{10}\frac{1}{\delta^2_{\hat{f}}}, dB \tag{14}$$

where $\gamma = g$ for direct observation and $\gamma = f^k$ for the restored image. Numerous experiments established the optimal parameters of the proposed influence function $\theta = 35, \upsilon = 5$, i.e. that gives the best compromise between impulse noise suppression and image degradation caused by decrease of the residual dynamic range. The 256×256 low-contrast test image "Minefield" was chosen (Figure 5a). Two types of objects were used in this image: circular "false" objects and "mines" which were modeled by the same circular structure with a low-contrast "hat" inside. This image was blurred by an antenna system with ratio of maximum image spatial frequency to antenna cut-off frequency of 2, with uniform field distribution over the aperture. Additive zero-mean Gaussian noise was added to the blurred image to obtain SNR 25 dB and the resultant image corrupted by salt-and-pepper impulse noise with p=0.3 (Figure 5b) and p=0.6 (Figure 5c). The results of median filtering, with window size L=5 for the image from Figure 5b and L=11 for the image from Figure 5c, are shown in Figure 5d, g, respectively. Such windows were chosen to completely eliminate impulse noise from the above images which could lead to false object detection. Due to the choice of large windows, caused by this requirement, and the noncompensated influence of the antenna system, the resultant images are characterized by poor resolution. Noise visibility functions, used further for the first iteration in our proposed restoration algorithm, were calculated from the median filtered images and for comparison are depicted in Figure 5e, h. Obviously, poor resolution caused a high level of ambiguity in the mine classification task. The application of the new algorithm to the restoration of images from Figure 5b, c is shown in Figure 5f, i, respectively. These images are obtained after 30 iterations with $\alpha = 0.01$. The images obtained have better quality and demonstrate high robustness of the proposed algorithm to impulse noise (see TABLE 1). During restoration, adaptation based on the proposed noise visibility function was performed. To compare the level of coincidence between the noise visibility function calculated from original image and the noise visibility functions used during restoration, the corresponding images are shown in Figure 5j, k, l. The results demonstrate an excellent match.

TABLE 1 - Comparison based on SNR between various methods in robust estimation schemes

Impulse noise (p)	Direct observation	Median filtering	Proposed method
30%	4.8 dB	25.8 dB	30.2 dB
60%	1.9 dB	24.2 dB	28.6 dB

This comparative analysis indicates the effectiveness of the proposed approach in terms of its robust features which give an increased probability of mine detection from low-resolution noisy images, and the discrimination of the detected objects among objects with similar geometry and dimensions.

REFERENCES

1. Press, W, Flannery, B, Teukolsky, S, and Vetterling, W, 1992, "Numerical Recipes: The Art of Scientific Computing", Cambridge University Press, Cambridge, UK

2. Voloshynovskiy S, Grytskiv Z, Allen A R, 1998, "High resolution radar imaging systems with robust image restoration", Proc. XII International Microwave & Radar Conference "MIKON'98", Krakow, Poland, 3, 876-880

3. Hrytskiv Z, Voloshynovskiy S, 1998, "Nonlinear adaptive-parametric image restoration", Int. J. of Machine Graphics & Vision, 7, 445-454

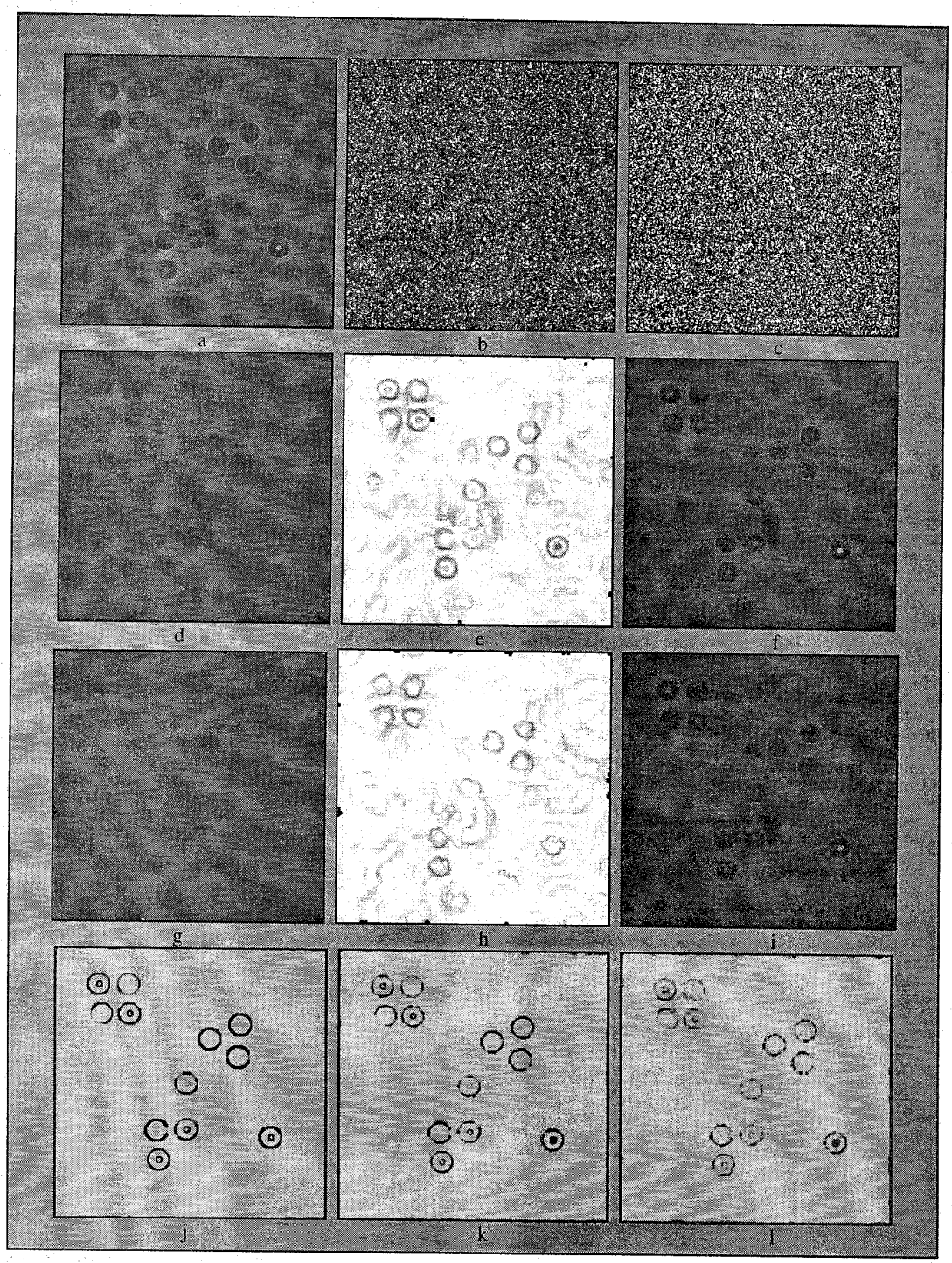

Figure 5: Results of computer simulation: (a) original "Minefield" image; (b) blurred and noisy image (a) with 25 dB additive Gaussian noise and 30% impulse noise; (c) blurred and noisy image (a) with 25 dB additive Gaussian noise and 60% impulse noise; (d) and (g) results of median filtering applied to images (b) and (c), respectively; (e) and (h) noise visibility functions obtained from median filtered images; (f) and (i) results of restoration by means of the proposed algorithm after 30 iterations for images (b) and (c) respectively; (j), (k) and (l) noise visibility functions calculated from original image (a), and restored images (f) and (i), respectively